

Thermal Hybrid Exchange-Correlation Density Functional for Improving the Description of Warm Dense Matter

D. I. Mihaylov, V. V. Karasiev, and S. X. Hu

Laboratory for Laser Energetics, University of Rochester

The warm-dense-matter (WDM) regime is too hot for standard condensed-matter approaches; however, quantum many-body effects are strong and classical plasma physics are not applicable. An established standard approach for accurate treatment of WDM is *ab initio* molecular dynamics (AIMD), when classical treatment for ions is combined with finite-temperature density functional theory (FT-DFT) for electronic degrees of freedom. Currently, all available exchange-correlation (XC) functionals in commonly used DFT software packages are ground-state functionals that do not explicitly depend on T but are evaluated at the T -dependent self-consistent density, i.e., $F_{XC}[n(T), T] \approx E_{XC}[n(T)]$ —an approach known as the ground-state approximation (GSA). Previously developed thermal functionals belong to the local density approximation (LDA) and generalized gradient approximation (GGA) level of refinement. At the LDA level, Karasiev *et al.* developed the nonempirical, thermal functional KSDT¹ (and its corrected version, corrKSDT; see Ref. 2), which is based on parameterized path-integral Monte Carlo data for the homogeneous electron gas at finite T and, in the zero- T limit, reduces to the ground-state Perdew–Zunger (PZ) functional. Subsequently, driven by the need to incorporate density-gradient effects and thereby account for the nonhomogeneity of the system, Karasiev *et al.* developed the GGA-level thermal functional KDT16 (Ref. 2) by analyzing the gradient expansion of weakly inhomogeneous electrons at finite T and defining appropriate T -dependent reduced variables for X and C . KDT16 is, by construction, nonempirical and reduces to the popular Perdew–Burke–Ernzerhof (PBE) functional in the zero- T limit. An example of the improved accuracy provided by the KDT16 functional was recently reported in Ref. 3, where KDT16-based AIMD studies of shocked deuterium showed improved agreement with experimental measurements of Hugoniot, reflectivity, and dc conductivity at elevated T . While it is clear that corrKSDT and KDT16 provide an apparent improvement over their ground-state counterparts PZ and PBE, they suffer from an inherent fundamental drawback—underestimating the electronic band gap. Hybrid XC functionals such as PBE0⁴ are constructed by mixing DFT XC functionals with Hartree–Fock (HF) exact exchange (EXX) and are known to be superior to GGA’s in predicting quantities such as E_{gap} , atomization energy, bond length, and vibrational frequency. In this work we present the KDT0 thermal hybrid model, which is based on a mixture of finite- T HF X and thermal KDT16 GGA XC:

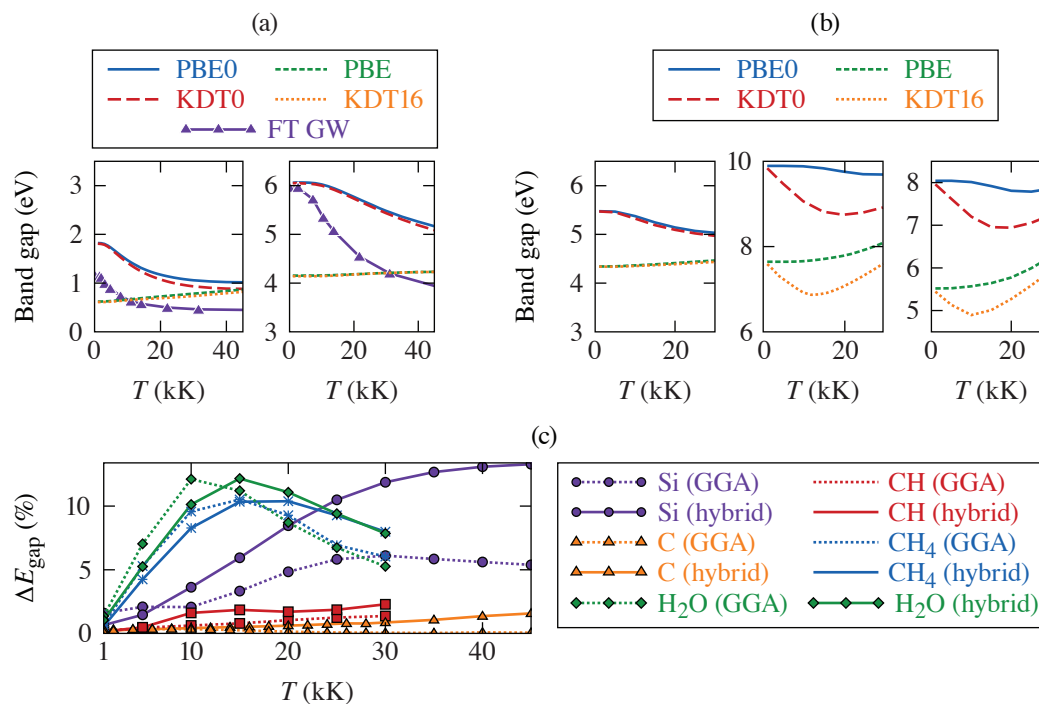
$$F_{XC}^{\text{hyb}}[n, T] = F_{XC}^{\text{DFA}}[n, T] + a(F_X^{\text{HF}}[n, T] - F_X^{\text{DFA}}[n, T]),$$

where $F_{X[C]}^{\text{DFA}}[n, T]$ is the KDT16 $X[C]$ free-energy density functional, $F_X^{\text{HF}}[n, T]$ is HF EXX free energy, and $a = 1/4$ is a parameter that is rationalized in Ref. 4 and gives a zero- T limit consistent with the PBE0 model. To compare performance between KDT0 and PBE0, we perform static calculations of the band gap as a function of electronic temperature $E_{\text{gap}}(T)$ when the positions of ions are fixed at near-ambient conditions. This corresponds to a two-temperature model, cold ions $T_i \approx 0$ K, and T is temperature of electrons $T_e = T$. The systems of choice are Si, C, CH₄, polystyrene (CH), and H₂O. The choice of Si and C was motivated by the need to compare the KDT0 functional to the highly accurate finite- T *GW* (Ref. 5) (FT *GW*) calculations, which is a high-precision, first-principles, many-body perturbation theory approach but is prohibitively expensive for AIMD. CH, CH₄, and H₂O calculations were performed so that our choice of model systems spans a wide range of densities and magnitudes for the zero- T gaps and also due to their relevance to high-energy-density physics (HEDP) and planetary science.

Figure 1 shows $E_{\text{gap}}(T)$ results for Si and diamond, which are two of the systems addressed in Ref. 5. Let us first compare the GSA functionals PBE and PBE0 in the case of Si. At low T , they both give an approximately equally wrong value for the

$E_{\text{gap}}(T)$, with PBE underestimating it and PBE0 overestimating it. At higher T , PBE0 predicts the same qualitative behavior as FT GW , monotonically decreasing $E_{\text{gap}}(T)$, while PBE predicts a monotonically increasing $E_{\text{gap}}(T)$, which is in direct contrast with FT GW predictions. The correct qualitative trend for $E_{\text{gap}}(T)$ predicted by PBE0 is a direct result of including T effects in XC through the T -dependent HF X and serves as an indication of the importance of thermal effects in XC. The same improvement in the qualitative behavior of $E_{\text{gap}}(T)$ provided by PBE0 is seen in diamond [Fig. 1(a) right]. Next, we turn our attention to results obtained with the thermal functionals KDT16 and KDT0. Most importantly, in both systems thermal XC effects lower the $E_{\text{gap}}(T)$ curve toward the more-accurate FT GW results, thereby improving qualitative behavior for all temperatures considered. We stress, however, two important observations: (1) the thermal corrections are strongly system dependent, with the relative difference in the gaps predicted by PBE0 and KDT0 reaching a maximum of 12.7% in Si and only 1.5% in diamond at $T = 45$ kK [see Fig. 1(c)]; (2) $\Delta E_{\text{gap}}(T)$ for hybrid-level functionals is larger than that for GGA's, which is a result of the different treatment of thermal effects in the X interaction between the hybrid and GGA levels of approximation. Motivated by these observations, we apply KDT0 and KDT16 to other systems of drastically different properties, such as density ρ and E_{gap} at near-ambient conditions. Results for $E_{\text{gap}}(T)$ in CH, CH₄, and H₂O for T up to 30 kK are shown in Fig. 1(b). In CH, $\rho = 1.06$ g/cm³, relative differences in $E_{\text{gap}}(T)$ predicted by PBE0 and KDT0 [see Fig. 1(b)] are small (<2.5%) and comparable to those in diamond. For CH₄, $\rho = 0.43$ g/cm³, and for H₂O, $\rho = 0.96$ g/cm³; $\Delta E_{\text{gap}}(T)$ reaches values comparable to those in Si at 45 kK, although the peaks occur at much lower T .

In conclusion, we have presented a thermal hybrid XC functional based on the KDT16 GGA XC free-energy density as density functional approximation for X and C free-energy terms and thermal HF X free energy, which leads to a finite- T extension of the PBE0 model, named here KDT0. Results for $E_{\text{gap}}(T)$ in various systems of interest to HEDP show that KDT16 could provide significant improvement to calculations of electronic properties for T within the WDM regime. We also see significant thermal



TC15407JR

Figure 1

(a) Band gaps of Si (left) and diamond (right) as a function of electronic temperature calculated with ground-state PBE and PBE0 and thermal KDT16 and KDT0 functionals. The green curve (FT GW) was extracted from Ref. 5. (b) Band gaps as a function of electronic temperature calculated with thermal (KDT0 and KDT16) and ground-state (PBE0 and PBE) functionals. (c) Relative difference between $E_{\text{gap}}(T)$ predicted by GSA and thermal XC. Dotted lines correspond to GGA-level, and solid lines correspond to hybrid-level thermal corrections. Colors correspond to different systems, the absolute values of the gaps for which are shown in (a) and (b).

XC effects on the entire band structure of studied systems, meaning that the accuracy of optic properties calculated via the Kubo–Greenwood formalism depends on accounting for those effects via thermal hybrid XC functionals. Also, we show that the importance of XC thermal effects depends strongly on the type of system and T range and that taking XC thermal effects into account at the hybrid level of approximation can lead to larger corrections compared to those at the GGA level, which further warrants the need for the development of advanced thermal *free-energy* density functionals.

This material is based upon work supported by the U.S. Department of Energy National Nuclear Security Administration under Award Number DE-NA0003856 and U.S. National Science Foundation PHY Grant No. 1802964. This research used resources of the National Energy Research Scientific Computing Center, a DOE Office of the Science User Facility supported by the Office of Science of the U.S. Department of Energy under Contract No. DE-AC02-05CH11231.

1. V. V. Karasiev *et al.*, Phys. Rev. Lett. **112**, 076403 (2014).
2. V. V. Karasiev, J. W. Dufty, and S. B. Trickey, Phys. Rev. Lett. **120**, 076401 (2018).
3. V. V. Karasiev *et al.*, Phys. Rev. B **99**, 214110 (2019).
4. J. P. Perdew, M. Ernzerhof, and K. Burke, J. Chem. Phys. **105**, 9982 (1996).
5. S. V. Faleev *et al.*, Phys. Rev. B **74**, 033101 (2006).